PAPER

Signal Quality Improvement in Downlink Power Domain NOMA with Blind Nonlinear Compensator and Frequency Domain Equalizer

Jun NAGAI[†a)], *Student Member*, Koji ISHIBASHI[†], *Senior Member*, *and* Yasushi YAMAO[†b)], *Fellow*

SUMMARY The non-orthogonal multiple access (NOMA) approach has been developed in the fifth-generation mobile communication systems (5G) and beyond, to improve the spectrum efficiency and accommodate a large number of IoT devices. Although power domain NOMA is a promising candidate, it is vulnerable to the nonlinearity of RF circuits and cannot achieve high-throughput transmission using high-level modulations in nonlinear environments. This study proposes a novel post-reception nonlinear compensation scheme consisting of two blind nonlinear compensators (BNLCs) and a frequency-domain equalizer (FDE) to reduce the effect of nonlinear distortion. The improvement possible with the proposed scheme is evaluated by using the error vector magnitude (EVM) of the received signal, which is obtained through computer simulations. The simulation results confirm that the proposed scheme can effectively improve the quality of the received downlink power-domain NOMA signal and enable high-throughput transmission under the transmitter (Tx) and receiver (Rx) nonlinearities via a frequency-selective fading channel.
key words: *5G, NOMA, SIC, nonlinear compensation, EVM*

1. Introduction

In recent years, novel mobile communication systems including 5G [1] and its beyond have been developed globally. These systems primarily aim to accommodate a large number of Internet of Things (IoT) devices along with the heavy traffic of broadband users. The non-orthogonal multiple access (NOMA) approach can improve the spectrum utilization of future systems by overlaying a large amount of IoT traffic on the broadband service traffic using the same radio resource [2].

Power domain NOMA [3] is a promising technique that exploits the difference of the received signal powers and the required data rates among the distributed users. The transmitter based on power domain NOMA multiplexes independent signal streams to the users via superposition, and the streams are decomposed at every user by employing a successive interference canceller (SIC) [4]. Various studies have demonstrated the effectiveness of NOMA in enhancing the spectrum utilization in downlink transmission [5].

However, the power domain NOMA systems face a major limitation due to the adverse impact of nonlinear distortions in the radio frequency (RF) circuits on the multiplexed signals [6], [7]. The signal for a user near the base station (BS) is assigned a small power as it differentiates the transmitting power for users based on their propagation loss and required SNR. However, the total transmitting power, including the far users, is still large, due to which the RF circuits in the BS transmitter or the receiver front-end of the near user may generate nonlinear distortions. It severely deteriorates the near-user signal with small power, which becomes evident when the SIC removes the large-power signal.

In order to mitigate the impact of nonlinear distortion and bring out full potential of NOMA, introduction of a nonlinear compensation (NLC) scheme is promising. In general, there are two approaches in NLC techniques. One is the transmitter NLC (Tx-NLC), such as digital predistortion (DPD) technique [8]. The other is the receiver NLC (Rx-NLC), which compensates nonlinearity after reception [7], [9]–[14]. Comparing two approaches from the point of signal transmission quality, Tx-NLC can compensate nonlinearity of the transmitter and suppress unnecessary emission to the adjacent channel. However, it cannot reduce nonlinear distortion generated in the receiver, which is serious in power domain NOMA environments. Therefore, employing Tx-NLC only is insufficient for the goal. On the other hand, although Rx-NLC was originally studied for compensating receiver nonlinearity, it has potential to compensate nonlinearities generated in both transmitter (Tx) and receiver (Rx) at the same time [14]. This is advantageous for achieving high-quality signal transmission required for NOMA when the spurious emission regulation is not strict. Moreover, optimized combination of Tx-NLC and Rx-NLC will achieve super-linear signal quality with low adjacent channel emission.

In ref. [7], an Rx-NLC method for NOMA system was proposed. In this method, the receiver demodulates the strong signal for the far user and this signal is used to estimate the nonlinear distortion. The bit error rate (BER) performance can be improved by subtracting the estimated distortion from the received signal. However, the estimation of the nonlinear distortion performed in this method is insufficient because it does not consider the cross-modulation of the far-user and near-user signals. This generates another distortion component that cannot be compensated by this

Manuscript received June 16, 2021.
Manuscript revised October 8, 2021.
Manuscript publicized December 1, 2021.
[†]The authors are with Advanced Wireless Communication & Research Center, The University of Electro-Communications, Chofu-shi, 182-8585 Japan.
a) E-mail: j.nagai@awcc.uec.ac.jp
b) E-mail: yyamao@m.ieice.org
DOI: 10.1587/transcom.2021EBT0003

method.

More promising solution is the blind nonlinear compensator (BNLC) [9]–[14]. It can compensate for all the nonlinear distortions, including the cross-modulation components, by using a polynomial-based nonlinear compensator. It does not require additional signal information to determine the compensator coefficients, apart from the bandwidth and center frequency. Therefore, BNLC can be widely applied to many systems because it is independent from modulations schemes and signal formats. Its performance against nonlinearity of Rx circuit has been presented under the flat Rayleigh fading propagation environments [12]. A basic study was conducted by applying the BNLC to NOMA in Ref. [13]. It is also suggested that the nonlinearity of both Tx and Rx can be compensated, for example, by expanding the polynomial model to include the Tx nonlinearity and by considering the propagation channel gain [14]. Therefore, BNLC-based scheme is considered to be the most attractive solution for the goal.

However, to achieve the Tx nonlinearity compensation in actual environments, the frequency selectivity of radio propagation channel gain must be considered as it causes waveform distortion, and the waveform of the resultant signal differs from that of the transmitted signal. When nonlinear compensation is performed in the receiver through such environment, the compensation performance changes and is not always successful.

Therefore, this paper proposes a novel solution to mitigate the effects of nonlinear distortion on the downlink power domain NOMA using the BNLC and the frequency-domain equalizer (FDE). In the solution, the propagation channel equalization and the nonlinear compensation are separated in a configuration with two BNLCs and an inter-BNLC FDE. The improvement presented by the proposed scheme is evaluated by the error vector magnitude (EVM) of the received signal. The computer simulation results confirm that the proposed method can effectively improve the quality of the received NOMA signal and enable high-throughput NOMA transmission under the Tx and Rx nonlinearities via a frequency-selective fading channel.

The remainder of this paper is organized as follows. Section 2 explains the downlink power-domain NOMA system and its issues. Section 3 presents the principle of the BNLC, which is followed by a discussion of the effect of the frequency-selective channel on nonlinear distortion in Sect. 4. In Sect. 5, a hybrid scheme consisting of two BNLCs and an inter-BNLC FDE is proposed. This is evaluated in Sect. 6 through computer simulations assuming a downlink NOMA environment. The conclusions of the study are presented in Sect. 7.

2. Effect of RF Circuit Nonlinearity in NOMA

In [6], the effect caused by nonlinear amplifiers is quantified as the degradation of the EVM, and the reception performance of the downlink NOMA for two user equipment (UE) is evaluated. Figure 1 shows the system model of the

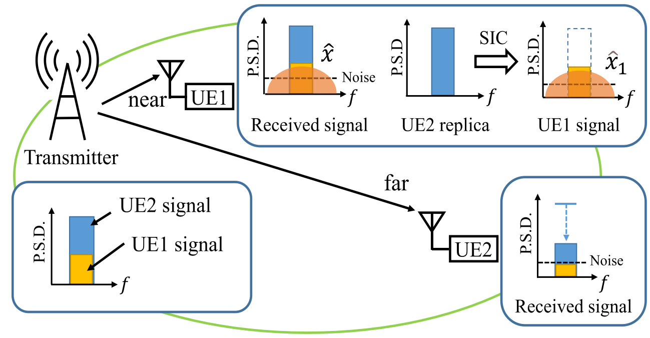

Fig. 1 System model for downlink power domain NOMA.

downlink power-domain NOMA when there are two UEs. UE1 is close to a base station (BS), whereas UE2 is far from the BS. The signals transmitted to UE1 and UE2 are $x_1(t)$ and $x_2(t)$, respectively. The power domain NOMA differentiates the transmitting power for the UEs as the propagation loss values vary significantly among the users based on their location. Based on the amplitude weight ratio,propagation loss values vary significantly among the users based on their location. Based on the amplitude weight ratio,c, the NOMA signal, x is expressed as[†]

$$x = cx_1 + (1 - c)x_2, \quad 0 < c < 0.5. \tag{1}$$

Here, the peak transmitting power of x_1 and x_2 in a subcarrier is assumed equal. Considering the propagation loss difference between the UEs, the weight, c, is determined such that the amplitude weight for UE1 is smaller than that for UE2. If UE1 is close to the BS, high throughput can be obtained by increasing the number of modulation levels, such as 64 quadrature amplitude modulation (QAM) and 256 QAM even for a small value of c. After the UE1 receiver creates a replica of the UE2 signal by demodulating the larger signal x_2, it subtracts the replica from the receiver output signal, $\hat{x}$. If $\hat{x}$ is affected by nonlinear distortion, the resultant signal, $\hat{x}_1$, deteriorates significantly due to the distortion, as shown in the figure. Consider,

$$\hat{x} = x + \rho, \tag{2}$$

where ρ is the nonlinear distortion with an averaged relative power level of l.

$$l = \frac{\overline{\rho^2}}{\overline{x^2}} \tag{3}$$

After the UE2 signal replica is subtracted, $\hat{x}_1$ is given as:

$$\hat{x}_1 = cx_1 + \rho. \tag{4}$$

The averaged relative distortion power level for x_1, l_1, increases from l as:

[†]Nonlinear distortion depends on the amplitude of input signal. For the NOMA system supposed in this paper, QAM signals are superpositioned in a subcarrier. Then the maximum amplitude of NOMA signal in the subcarrier is the sum of maximum amplitudes for two signals. Therefore, we set the condition that keeps the amplitude sum constant by using the amplitude weight ratio c.

$$l_1 = \frac{\overline{\rho^2}}{c^2\overline{x_1^2}} = \frac{c^2\overline{x_1^2} + (1-c)^2\overline{x_2^2}}{c^2\overline{x_1^2}} l > l. \tag{5}$$

To obtain the above equation, we assume the stochastic independence between x_1 and x_2. Consequently, the EVM of $\hat{x}_1$ increases considerably, and the BER performance is severely deteriorated. Therefore, reducing the nonlinear distortion and suppressing the degradation of multiplexed signals in the downlink power domain NOMA is crucial. This study introduces the BNLC and FDE to mitigate the effects of nonlinear distortion.

3. Blind Nonlinear Compensator (BNLC)

Firstly, the basic nonlinear compensation by the BNLC is considered. Figure 2 shows the block diagram of the BNLC, which is a post-reception nonlinear compensator. It is assumed that the transmitted signal is unknown and the only information available is bandwidth and center frequency of the signal. Nonlinear distortion is assumed to occur either on the receiver or the transmitter, or both.

Typically, nonlinearity in the input/output characteristic of an RF circuit is expressed as an equivalent baseband polynomial [15]:

$$y = \sum_{\substack{p=1\\\text{odd}}}^{P} a_p |x|^{p-1} x, \tag{6}$$

where x and y are the nonlinear circuit input/output signals in the continuous-time domain, P is the maximum order of nonlinearity, a_p is the p_{th} order nonlinear coefficient, and x, y, and a_p are complex numbers.

Consider the nonlinear output, y, in Eq. (6) as the input to the BNLC. The polynomial form can also be used for a nonlinear compensator to realize an inverse characteristic of the circuit. The input/output characteristics of the compensator are given by:

$$z = \sum_{\substack{q=1\\\text{odd}}}^{Q} b_q |y|^{q-1} y, \tag{7}$$

where y and z are the compensator input/output signals in the continuous-time domain, Q is the maximum order of nonlinear compensation, and b_q is the q_{th} order compensator coefficient. Q must be equal to or higher than P to achieve high-accuracy compensation.

A nonlinearity of RF circuit device creates both in-band and outband distortion components. Although it is difficult to measure in-band distortion power from the unknown input signal, the outband radiation power can be easily measured if the signal bandwidth is known. Since the in-band distortion power is highly correlated to the outband distortion power, we can minimize the total distortion power by minimizing the outband distortion power. Based on this property, the BNLC determines the coefficient, b_q, that can

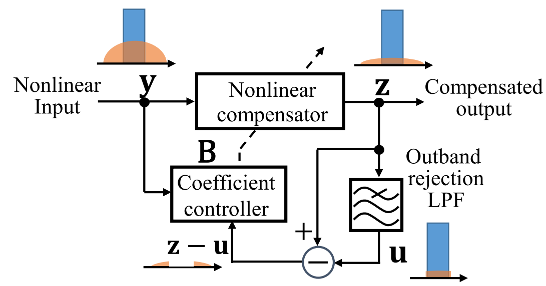

Fig. 2 Block diagram of BNLC.

minimize the outband radiation power [9], [10]. The output signal, $u(t)$, from the outband rejection low-pass filter (LPF) in the figure is represented as:

$$u = h_{\text{LPF}} * z, \tag{8}$$

where h_{LPF} is the impulse response of the outband-rejection LPF with the bandwidth of the original signal and $*$ represents the convolution of two time-domain signals. The outband nonlinear distortion component is obtained by subtracting u from z. The outband rejection LPF must have flat response throughout the signal band and sharp cutoff characteristic for the outband.

Consider the BNLC, which processes discrete-time digital signals in the equivalent baseband. Here, y, z, and u are replaced by sample vectors, such that:

$$\mathbf{y} = [y_1, y_2, \ldots, y_l, \ldots, y_L]^{\mathrm{T}}, \tag{9}$$
$$\mathbf{z} = [z_1, z_2, \ldots, z_l, \ldots, z_L]^{\mathrm{T}}, \tag{10}$$
$$\mathbf{u} = [u_1, u_2, \ldots, u_l, \ldots, u_L]^{\mathrm{T}}, \tag{11}$$

where L is the number of signal samples in a unit processing block. Equation (7) can then be expressed in the discrete-time domain as:

$$\mathbf{z} = \mathbf{K}_Q(\mathbf{y})\mathbf{B}, \tag{12}$$

$$\mathbf{K}_Q(\mathbf{y}) = \begin{bmatrix} y_1 & |y_1|^2 y_1 & \cdots & |y_1|^{Q-1} y_1 \\ y_2 & |y_2|^2 y_2 & \ddots & |y_2|^{Q-1} y_2 \\ \vdots & \vdots & & \vdots \\ y_L & |y_L|^2 y_L & \cdots & |y_L|^{Q-1} y_L \end{bmatrix}, \tag{13}$$

$$\mathbf{B} = \left[b_1, b_3, \ldots, b_q, \ldots, b_Q\right]^{\mathrm{T}}, \tag{14}$$

where $\mathbf{K}_Q(\mathbf{y})$ is the kernel matrix of the inverse characteristic polynomial of $L \times (Q+1)/2$ and $\mathbf{B}$ is the compensator coefficient vector. From the equations defined above, the outband signal power can be represented as:

$$\begin{aligned} P_{\text{out}} &= \sum_{l=1}^{L} |z_l - u_l|^2 \\ &= \|\mathbf{z} - \mathbf{u}\|^2 \\ &= \left\|\mathbf{K}_Q(\mathbf{y})\mathbf{B} - \mathbf{u}\right\|^2. \end{aligned} \tag{15}$$

$\mathbf{B}$ can be determined to minimize the outband signal power using the least square (LS) method and can be defined as:

$$\mathbf{B} = \left(\mathbf{K}_Q^{\mathrm{H}}(\mathbf{y})\mathbf{K}_Q(\mathbf{y})\right)^{-1}\mathbf{K}_Q^{\mathrm{H}}(\mathbf{y})\mathbf{u}. \tag{16}$$

4. Effect of Frequency-Selectivity of Radio Propagation Channel on Post-Reception Nonlinear Compensation

The unit RF signal bandwidth of the mobile communication systems has increased to enhance the system capacity and achieve high throughput. The wideband propagation channels exhibit frequency selectivity due to multipath fading. Thus, a transmitted signal with nonlinear distortion channels exhibit frequency selectivity due to multipath fading. Thus, a transmitted signal with nonlinear distortion is affected by the frequency-selective channel. This section discusses the interaction between the post-reception nonlinear compensation and the equalization of the radio propagation channel.

The wideband propagation channel causes waveform distortion that is modeled by a linear filter with a transfer function of the channel. This waveform distortion can be equalized by FDE using pilot signals inserted into the transmitted signal. For example, both the orthogonal frequency division multiplexing (OFDM) and single-carrier frequency division multiple access (SC-FDMA) signals in the LTE-Advanced and 5G systems periodically insert multiple pilot signals in both the time and frequency domains [16] to enable channel equalization. They employ low-level modulation for tolerating noise and nonlinearity.

Figure 3 shows the concept of combining post-reception nonlinear compensation with the FDE. In the figure, the Rx-NLM and Tx-NLM represent a receiver nonlinear circuit model and a transmitter nonlinear circuit model, respectively. H is the transfer function of the frequency-selective radio channel. The transfer function of the FDE is H^{-1}, which is the inverse of the transfer function of the radio channel. In (a), the BNLC is placed immediately after the receiver and can perform the receiver nonlinearity compensation independent of radio channel characteristics. The FDE can then perform channel equalization after the nonlinearity has been removed.

Conversely, when nonlinear distortion is generated at the transmitter as shown in (b), the receiver input waveform is modified from the transmitted signal due to the frequency-selective radio channel. In this case, the post-reception nonlinear compensation is unsuccessful with the receiver configuration shown in Fig. 3(a). To overcome this issue, the order of the BNLC and FDE must be changed as shown in Fig. 3(b). The BNLC can compensate for the Tx nonlinearity regardless of the channel characteristics by first performing channel equalization.

Unfortunately, both configurations are dedicated to the nonlinear compensation of one side, i.e., either Tx or Rx, and cannot simultaneously handle the Tx and Rx nonlinearities. Therefore, another compensation scheme must be identified that can simultaneously handle both nonlinearities via a frequency-selective propagation channel.

(a) Compensating for receiver nonlinearity.

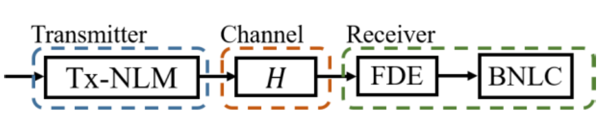

(b) Compensating for transmitter nonlinearity.

Fig. 3 Nonlinear compensation with radio propagation channel.

5. Hybrid Nonlinear Compensation Scheme with Multiple BNLCs and FDE

This section proposes a new post-reception nonlinear compensation scheme that comprises two BNLCs and an FDE connected in series. It can compensate for the nonlinear distortions generated by the transmitter and receiver connected via a frequency-selective propagation channel.

Figure 4 shows the signal-processing block diagram of the proposed scheme. The transmitted signal is affected by the Tx-NLM, frequency-selective channel, and Rx-NLM in series. In the figure, the transfer function of the FDE is H^{-1}, which is the inverse characteristic of the frequency-selective propagation channel.

From the order of processing blocks, it is ideal that BNLC_1 first compensates for Rx-NLM, and BNLC_2 compensates for Tx-NLM after equalizing the frequency-selective channel. However, this is not possible because the nonlinear coefficients of Tx-NLM and Rx-NLM cannot be completely separated at the receiver side. In practice, BNLC_1 first identifies the coefficients of Rx-NLM that are unaffected by the frequency-selective channel and removes this distortion; the effect of the frequency-selective channel is then removed by the FDE, and the remaining nonlinear distortion which is mainly obtained from Tx-NLM is identified by BNLC_2 and removed. Essentially, the compensation of the combined nonlinearity is conducted in two stages. Therefore, this approach provides a practical solution rather than the perfect solution for the tandem nonlinearity via frequency-selective channel.

When compared to the scheme in Ref. [14], which employs a single BNLC with a tandem nonlinear model, the aim of the proposed scheme is similar in terms of simultaneously compensating the nonlinearities of the Tx and Rx. However, the effectiveness of this scheme has been confirmed only for the flat fading channels and not for the

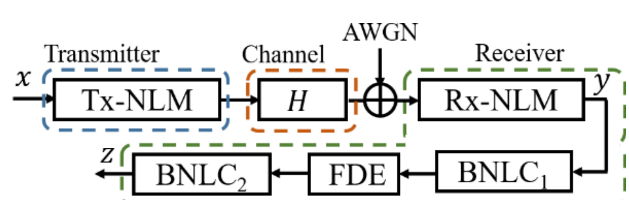

Fig. 4 Signal processing block diagram of proposed scheme.

frequency-selective channels. The propagation channel gain constant, h, in the tandem nonlinear model must be transformed to an impulse response form to cover the frequency-selective fading channels with this scheme. This implies that the tandem nonlinearity model must be extended to a memory polynomial form. In this case, the number of coefficients to be determined by the compensator increases based on the product of the joint nonlinear order for the Tx and Rx, and the impulse response length. For example, consider that the maximum nonlinear order is three (the minimum value) for both the Tx and Rx, and that the number of coefficients in the tandem nonlinear model is set nine [14]. When the scheme is extended to the memory polynomial form [8], the number of polynomial coefficients is multiplied by the impulse response length in the samples or by its power, resulting in a large number.

The necessary impulse response length depends on the delay spread of the fading channel and the channel bandwidth. For example, the 3GPP extended pedestrian-A (EPA) model [16] specifies a seven-path model with a maximum delay spread of 410 ns. Assuming a 20 MHz LTE-Advanced channel, the required signal sampling frequency in the baseband is approximately 60 MHz, considering the IM3 distortion. In this example, an impulse response length of 25 stages is required to cover the delay spread. Thus, the required number of tandem model coefficients is multiplied by 25 and results in 225 when using the memory polynomial model in Ref. [17].

On the other hand, the proposed scheme separates nonlinear compensation and channel equalization. Consequently, the number of coefficients to be determined is the sum of BNLC_1, FDE, and BNLC_2. For the same delay spread condition as that of the tandem model, $5+25+5 = 35$ coefficients are required for the proposed scheme, which is less than 1/6th of the tandem nonlinear models. Therefore, this scheme significantly reduces the amount of calculation, reduces the convergence time, and enables greater stability of operation in fast-fading environments.

Even if the large number of coefficients are successfully determined in the extended tandem nonlinear model, another issue is known that nonlinear compensation performance with the memory polynomial model is not better [18] when the frequency-selectivity is severe. From the author's other study results, EVM performance with the memory polynomial model is not better than single BNLC+FDE [19].

Other precise memory models, such as the generalized memory polynomial model [18], may be necessary for the tandem nonlinear modeling. In this case, the number of coefficients increases further, requiring a huge number of samples to accurately determine the coefficients. However, collecting a large number of samples requires considerable time and increases the difficulty in tracking the fast-fading channels and updating the compensation coefficients. Therefore, compressing the number of coefficients in the generalized memory polynomial model is an important issue that remains as the future work.

6. Performance Evaluation by Simulations

6.1 Simulation Model and Settings

Consider the downlink two-user power-domain NOMA system in Fig. 1. Figure 5 shows a block diagram of the proposed NOMA receiver for UE1. A UE2 signal replica, x_2, is generated from the proposed nonlinear compensator output signal, z. It is then subtracted from z to regenerate the UE1 signal. The proposed nonlinear compensator consists of an FDE, and two BNLCs, i.e., BNLC_1 and BNLC_2, connected before and after the FDE. The two BNLCs compensate for nonlinearity independent of each other, such that the radiation power of each outband is minimized. A rectangular frequency response filter is realized by the fast Fourier transform (FFT) method in each processing block as the outband noise rejection LPF in Fig. 2. Pass bandwidth is set a little wider to signal bandwidth. The FDE contains the inverse transfer function of the radio channel.

The performance of the proposed nonlinear compensation scheme in the downlink NOMA transmission is evaluated through computer simulations using MATLAB. Table 1 lists the simulation conditions. The transmitting signals are LTE-A for both UE1 and UE2, and the modulation schemes used for UE1 and UE2 are 64QAM and quadrature phase shift keying (QPSK), respectively. The NOMA amplitude weight, c, is changed from 0.1 to 0.35. Both the flat Rayleigh fading channel model and the 3GPP-defined frequency-selective fading channel EPA model [16] are employed for evaluation and comparison. Fig. 6 presents the frequency response of the EPA channel path loss model at a center frequency of 2.25 GHz.

The Saleh model [20], which is a commonly used behavior model for microwave amplifiers, is used as the nonlinear input-output characteristic model of the RF circuit. The AM-AM and AM-PM characteristics are given by the following input/output functions:

$$\mathrm{AM/AM} = \frac{\alpha_A r}{1+\beta_A r^2}, \tag{17}$$

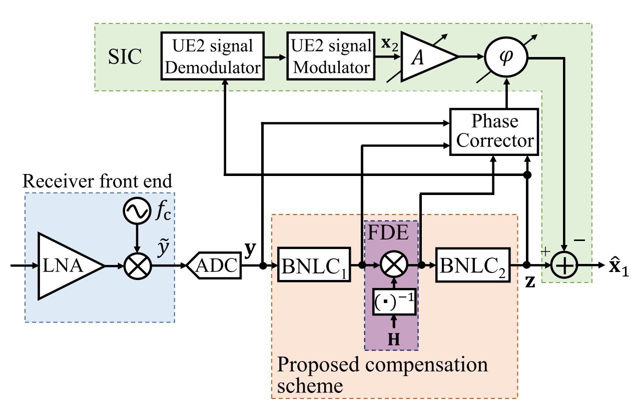

Fig. 5 Signal processing block diagram of UE1 receiver.

Table 1 System parameters.

	UE1	UE2
Transmitted signal	LTE-A / OFDM	
RF signal bandwidth	18.1 MHz	
Modulation scheme	64QAM	QPSK
NOMA amplitude weight	0.1 - 0.35	0.9 – 0.65
RF center frequency	2.25 GHz	
Chanel model	Flat Rayleigh fading model and EPA model	
Maximum Doppler frequency	5 Hz	
Nonlinear model for Tx and Rx	Saleh model	
Output backoff for NOMA signal	9 dB	
Sampling frequency	61.44 MHz	
Signal processing block size	4096 samples	
Max. order of compensation	5	
Number of coefficient updates	20 Max.	

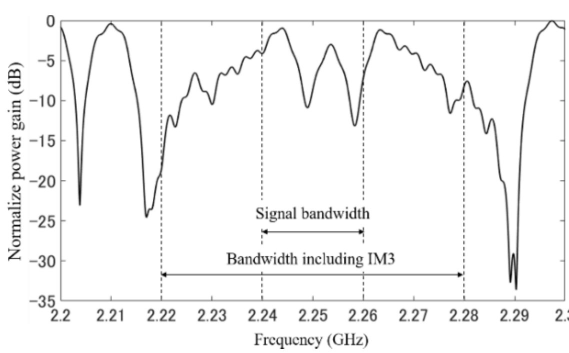

Fig. 6 Frequency response of EPA channel model.

$$\mathrm{AM/PM} = \frac{\alpha_P r^2}{1+\beta_P r^2}, \tag{18}$$

where r is the amplitude of input signal and $\alpha_{A,p}, \beta_{A,p}$ are the parameters that determine the nonlinear characteristics. In the simulation, $\alpha_A, \beta_A, \alpha_P$, and β_P are set to 2, 1, $-(\pi/3)$, and 1, respectively, as the typical values. The output back-off level for the Tx and Rx is set to 9 dB. Since the third-order nonlinearity is dominant in the Saleh model, the maximum order of compensators is set to five.

6.2 Performance in Flat Rayleigh Fading Environment

Figure 7 shows the distribution of signal constellation for the NOMA system with $c = 0.35$ via the flat fading channel. Without nonlinear compensation, the NOMA signal constellation in (a) is adversely affected by the device nonlinearity. This results in the contaminated UE1 signal in (b) after the UE2 signal replica is subtracted from the constellation (a). Nonlinear distortion is removed when the proposed scheme is added and the NOMA signal becomes clean, as shown in Fig. 7(c). The UE1 signal after the SIC shown in (d) is a 64QAM signal with low distortion.

The EVM for the received signals is calculated to quantify the signal quality. Figure 8 shows the EVM characteristic of UE1 corresponding to the amplitude weight ratio, c, under the flat Rayleigh fading environment. Without the BNLC, the EVM increases with the decrease in the

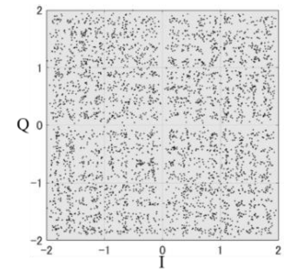

(a) NOMA signal w/o compensation

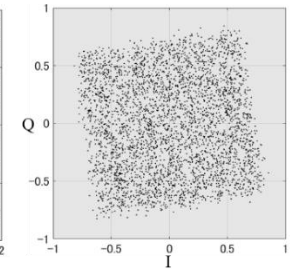

(b) UE1 signal after SIC w/o compensation

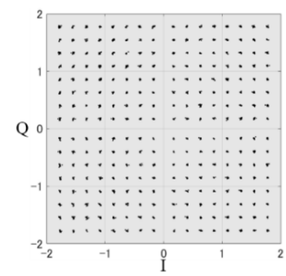

(c) NOMA signal with proposed scheme

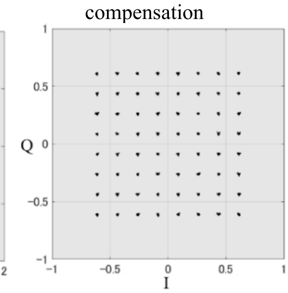

(d) UE1 signal after SIC with proposed scheme

Fig. 7 Signal constellations for $c = 0.35$ via flat fading channel.

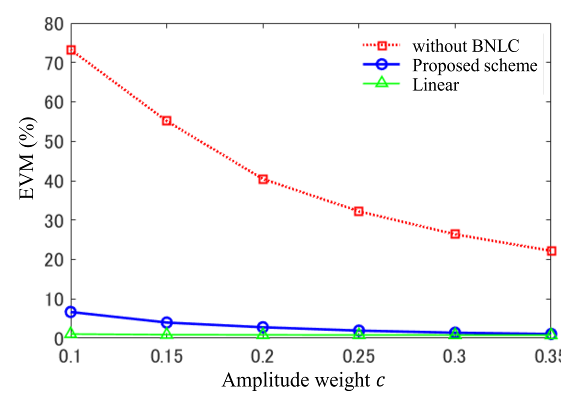

(a) UE1 EVM characteristics

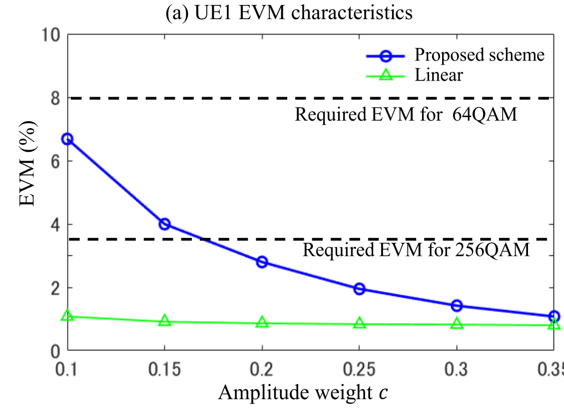

(b) Close view of (a) (EVM of 0 %–10%).

Fig. 8 UE1 EVM characteristics under flat fading environment.

NOMA amplitude weight, c. This is because the EVM for UE1 depends on c, as shown in Eq. (5). In Fig. 8(a), the EVM is remarkably improved by the proposed scheme for any amplitude weight c. In the detailed view in Fig. 8(b), the required EVM values defined in the 3GPP standard [16] are added by broken lines for reference, which are 8% and 3.5% for 64QAM and 256QAM, respectively. The simulated EVM values can satisfy the 64QAM requirement for all the amplitude ratios and satisfy the 256QAM requirement for $c = 0.17$ or greater.

Figure 8 also indicates "Linear" EVM plots as reference that shows the EVM measured without nonlinear device and BNLCs. Although the difference of EVM values between Linear and the proposed scheme is small when c is 0.35, it increases as c becomes smaller. It is due to the residual compensation error of BNLC, which influences much for smaller c. The same degradation is observed for the single BNLC with tandem nonlinear model in Ref. [14]. This scheme and the proposed scheme present similar performance in the flat fading environment.

6.3 Performance in Frequency-Selective Fading Environment

Figure 9 shows the distribution of the signal constellation for the NOMA system with $c = 0.35$ under the EPA channel model. It can be observed from Figs. 9(a) and (b), that the signals are adversely affected by the device nonlinearity and frequency-selective fading. With the proposed scheme, the nonlinearity under the EPA channel is effectively compensated as shown in Figs. 9(c) and (d). When compared to the results in Fig. 7, the signal constellations are spread more in Fig. 9(c) and (d), which indicates that the performance is degraded from the flat fading case in Fig. 7.

Figure 10 presents the EVM characteristics under the EPA channel model. It can be observed from Fig. 10(a) that EVM is severely deteriorated by both the device nonlinearity and frequency-selective fading when the BNLC and FDE are not used. The EVM is improved with the FDE, but it is insufficient when performed alone. The EVM is more than 20% for all the c values, which cannot satisfy the required EVMs. Even if a BNLC is added to the FDE, the EVM cannot be improved by either $BNLC_1$ or $BNLC_2$ alone. The single BNLC with tandem nonlinear model [14] also showed insufficient performance under frequency-selective fading environment. However, the proposed configuration with two BNLCs and the inter-BNLC FDE can effectively improve the EVM. In the detailed view shown in Fig. 10(b), it is observed the simulated EVM values for UE1 with the proposed scheme can satisfy the 64QAM EVM requirement for the values of c greater than 0.23. Although the required EVM value for 64QAM is difficult to achieve for values of c smaller than 0.23, it is confirmed that the proposed scheme enables high-throughput NOMA transmission under the Tx

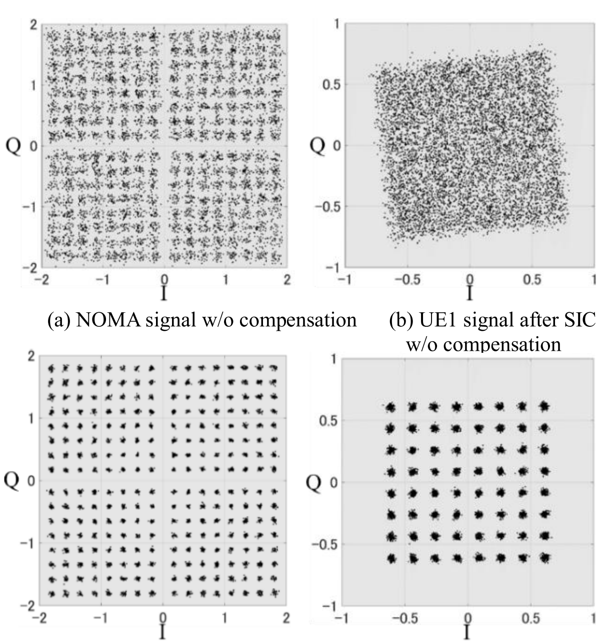

(a) NOMA signal w/o compensation
(b) UE1 signal after SIC w/o compensation
(c) NOMA signal with proposed scheme
(d) UE1 signal after SIC with proposed scheme

Fig. 9 Signal constellations via EPA channel.

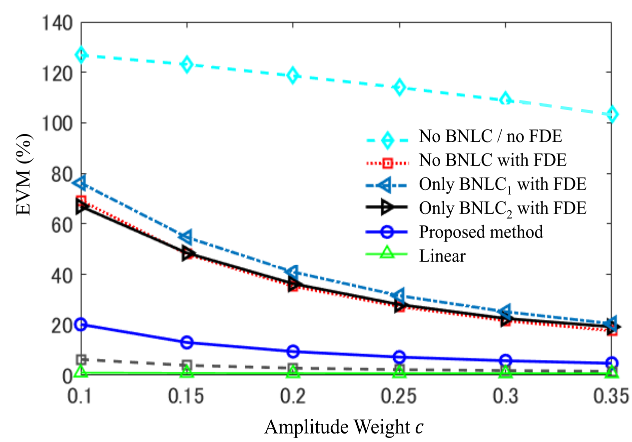

(a) UE1 EVM characteristic.

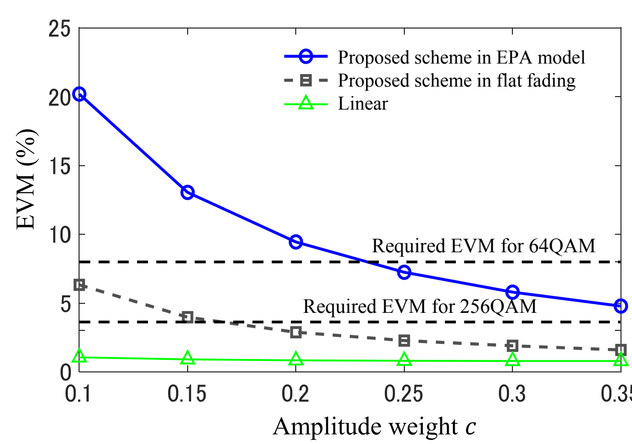

(b) Closed view of (a) (EVM of 0%–25%).

Fig. 10 UE1 EVM characteristics via EPA channel.

and Rx nonlinearities via a frequency-selective fading channel.

7. Conclusions

This study proposes an advanced solution that employs the BNLC and FDE to mitigate the severe effects of nonlinear distortion on the downlink power domain NOMA. In the solution, the frequency-selective channel equalization and nonlinear compensation are separated in a configuration with two BNLCs and an inter-BNLC FDE. The improvement presented by the proposed scheme is evaluated by the EVM of the received signal. Computer simulation results confirmed that the proposed method can effectively compensate nonlinear distortion and improve the quality of the received NOMA signal. It enables high-throughput NOMA transmission by using high-level modulation schemes such as 64QAM under the Tx and Rx nonlinearities via frequency-selective fading channels.

References

[1] C-X. Wang, F. Haider, X. Gao, X-H. You, Y. Yang, D. Yuan, H.M. Aggoune, H. Haas, S. Fletcher, and E. Hepsaydir, "Cellular architecture and key technologies for 5G wireless communication networks," IEEE Commun. Mag., vol.52, no.2, pp.122–130, Feb. 2014.

[2] A. Benjebbour, Y. Saito, Y. Kishiyama, A. Li, A. Harada, and T. Nakamura, "Concept and practical considerations of non-orthogonal multiple access (NOMA) for future radio access," Proc. ISPACS 2013, pp.770–774, Nov. 2013.

[3] A. Benjebbour, A. Li, Y. Saito, Y. Kishiyama, A. Harada, and T. Nakamura, "System-level performance of downlink NOMA for future LTE enhancements," Proc. IEEE Globecom 2013, Dec. 2013.

[4] S.M.R. Islam, N. Avazov, O. Dobre, and K.S. Kwak, "Power-domain non-orthogonal multiple access (NOMA) in 5G systems: Potentials and challenges," IEEE Commun. Surveys Tuts., vol.19, no.2, pp.721–742, Second quarter 2017.

[5] S. Tomida and K. Higuchi, "Non-orthogonal access with SIC in cellular downlink for user fairness enhancement," Proc. ISPACS 2011, Dec. 2011.

[6] K. Mayama, K. Akimoto, S. Kameda, and N. Suematsu, "Evaluation of reception performance considering error vector magnitude for downlink non-orthogonal multiple access," IEICE Technical Report, RCS2018-91, July 2018.

[7] J. Guerreiro, R. Dinis, P. Montezuma, and M.M. da Silva, "Nonlinear effects in NOMA signals: Performance evaluation and receiver design," Proc. IEEE VTC2019-Fall, pp.1–5, Sept. 2019.

[8] F.M. Ghannouchi and O. Hammi, "Behavioral modeling and predistortion," IEEE Microw. Mag., vol.10, no.7, pp.52–64, Dec. 2009.

[9] K. Dogancay, "Blind compensation of nonlinear distortion for bandlimited signals," IEEE Trans. Circuits Syst. I, Reg. Papers, vol.52, no.9, pp.1872–1882, Sept. 2005.

[10] Y. Ma and Y. Yamao, "Blind nonlinear compensation technique for RF receiver front-end," Proc. 43rd European Microwave Conf., pp.1527–1530, Nuremberg, Germany, Oct. 2013.

[11] Y. Ma, Y. Yamao, K. Ishibashi, and Y. Akaiwa, "Adaptive compensation of inter-band modulation distortion for tunable concurrent dual-band receivers," IEEE Trans. Microw. Theory. Techn., vol.61, no.12, pp.4209–4219, Dec. 2013.

[12] K. Kimura and Y. Yamao, "Bandwidth-efficient blind nonlinear compensation of RF receiver employing folded-spectrum sub-nyquist sampling technique," IEICE Trans. Commun., vol.E102-B, no.3, pp.632–640, March 2019.

[13] J. Nagai, T. Abe, and Y. Yamao, "Improvement of EVM for downlink NOMA with blind nonlinear compensation scheme," Proc. IEEE VTC2020-Spring, 1N-1, May, 2020.

[14] T. Abe and Y. Yamao, "Blind post-compensation of tandem nonlinearly caused by transmitter and receiver," Proc. IEEE RWS2020, pp.12–15, San Antonio, USA, Jan. 2020.

[15] R. Raich, H. Qian, and G.T. Zhou, "Orthogonal polynomials for power amplifier modeling and predistorter design," Proc. IEEE Trans. Veh. Technol., vol.53, no.5, pp.1468–1479, Sept. 2004.

[16] 3GPP TS 36.101. version 14.5.0 Release 14, "Evolved universal terrestrial radio access (E-UTRA); User equipment (UE) radio transmission and reception," 3rd Generation Partnership Project; Technical Specification Group Radio Access Network, pp.1332–1437, Nov. 2017.

[17] L. Ding, G.T. Zhou, D.R. Morgan, Z. Ma, J.S. Kenney, J. Kim, and C.R. Giardina, "A robust digital baseband predistorter constructed using memory polynomials," IEEE Trans. Commun., vol.52, no.1, pp.159–165, Jan. 2004.

[18] D.R. Morgan, Z. Ma, J. Kim, M.G. Zierdt, and J. Pastalan, "A generalized memory polynomial model for digital predistortion of RF power amplifiers," IEEE Trans. Signal Process., vol.54, no.10, pp.3852–3860, Sept. 2006.

[19] H. Ito, T. Fujii, and Y. Yamao, "Post-reception compensation performance of blind nonlinear compensator with equalizer against memory nonlinear distortion," Proc. IEEE VTC2020-Fall, Nov. 2020.

[20] A.M. Saleh, "Frequency-independent and frequency-dependent nonlinear models of TWT amplifiers," IEEE Trans. Commun., vol.29, no.11, pp.1715–1720, Nov. 1981.

Jun Nagai received the B.S. and M.S. degrees in Electrical Engineering from the University of Electro-Communications in 2019 and 2021, respectively. He is now working with NTT DoCoMo Inc.

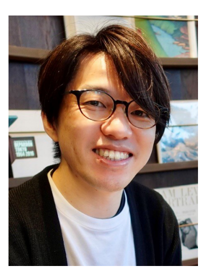

Koji Ishibashi received his B.E. and M.E. degrees from The University of Electro-Communications, Tokyo, Japan, in 2002 and 2004, respectively, and received his Ph.D. in engineering from Yokohama National University, Yokohama, Japan, in 2007. From 2007 to 2012, he was an assistant professor at the Department of Electrical and Electronic Engineering, Shizuoka University, Hamamatsu, Japan. Since April 2012, he has been working with the Advanced Wireless and Communication Research Center (AWCC), The University of Electro-Communications, Tokyo, Japan, where he is currently a professor. From 2010 to 2012, he was a visiting scholar at the School of Engineering and Applied Sciences, Harvard University, Cambridge, MA. His current research interests include grant-free access, cell-free architecture, millimeter-wave communications, energy harvesting communications, wireless power transfer, channel codes, signal processing, and information theory. He served as an associate editor of the IEICE Transactions on Communications from 2015 to 2020.

Yasushi Yamao received his B.S., M.S., and Ph.D. degrees in electronics engineering from Kyoto University, Kyoto, Japan, in 1977, 1979, and 1998, respectively. He began his research career in mobile communications in the measurement and analysis of urban radio propagation as his M.S. thesis. In 1979, he joined the Nippon Telegraph and Telephone Corporation (NTT) Laboratories, Japan, where his major activities included leading research on GMSK modulator/demodulator and GaAs RF ICs for digital mobile communications, and development of PDC digital cellular handheld phones. In 1993, he moved to NTT DoCoMo Inc. and directed the standardization of a high-speed paging system (FLEX-TD) and the development of a 3G radio network system. He also joined the European IST research programs for IP-based 4th generation mobile communication. In 2005, he moved to the University of Electro-Communications as a professor of the Advanced Wireless Communication Research Center (AWCC). His interests include wireless communication networks and protocols, as well as high-efficiency and reconfigurable wireless circuit technologies in both RF and Digital Signal Processing. Prof. Yamao is a Fellow of the IEICE, member of IPSJ and life member of the IEEE. He has served as the Vice President of the IEICE Communications Society (2003–2004), the Chairman of the IEICE Technical Group on Radio Communication Systems (2006–2008), the Chief Editor of IEICE Communication Magazine (2008–2010), the Vice chairman of IEEE VTS Japan chapter (2009–2015), and a Director of the IEICE (2015–2017). He is currently the Chairman of IEEE VTS Japan chapter (2019–)